SAND2011-4419C

Numerical study of radiatively induced entrainment

H Schmidt[1], A R Kerstein[2], R Nédélec[3], S Wunsch[4], and B J Sayler[5]

[1] Department of Mechanical Engineering, Technical University of Cottbus, Germany
[2] Combustion Research Facility, Sandia National Laboratories, USA
[3] Open Cascade S.A.S., Paris, France
[4] Applied Physics Laboratory, Johns Hopkins University, USA
[5] Black Hills State University, USA

E-mail: schmidth@tu-cottbus.de

Abstract. Numerical simulations using the one-dimensional turbulence (ODT) model are compared to water-tank measurements emulating convection and entrainment in stratiform clouds driven by cloud-top cooling. Measured dependences of the entrainment rate on Richardson number are reproduced. An additional parameter variation suggests more complicated dependences of the entrainment rate than previously anticipated. Uncertainties in the modeling assumptions and in the experimental results are discussed.

1. Introduction

Since entrainment in stratiform clouds is partly radiatively driven, a laboratory experiment involving this mechanism has been conducted (Sayler & Breidenthal, 1998). In particular, the case of entrainment across a capping temperature inversion and induced by *cloud top* cooling has been investigated. This geometry is termed interfacial convection, and its physics differ from the more thoroughly studied case of penetrative convection. The study builds upon a pioneering work (McEwan & Paltridge, 1976). The experimental setup is sketched in Fig. 1. A tank is filled with an aqueous fluid consisting of blue (opaque) and yellow (translucent) upper and lower layers, respectively. A stable density stratification is achieved between the two layers, whose intensity varies for each trial. In this paper we focus on the trials where the stratification is initialized by a temperature difference between the layers. The tank is lit from below with two sodium lamps to provoke an instability at the interface via radiative heating. The temperature and light flux are measured periodically in the tank. Dimensional entrainment rates and non-dimensional entrainment E have been calculated based on these measurements. Several parameters have been systematically varied during the experiment and it has been found that the non-dimensional entrainment rate varies like the inverse of the Richardson number. Finally, for five trials the optical depth of the upper (opaque) fluid has been varied and the results analyzed. This optical depth is a measure of the opacity of the fluid. Despite Reynolds numbers that differ by four orders of magnitude or more between the laboratory simulation and the real atmosphere, it is argued that the entrainment dynamics are analogous. Dimensionless entrainment rates measured in the laboratory were within one order of magnitude of those measured in the atmosphere for a given Richardson number. It was argued that thin Taylor layers and the lack of evaporative effects in the laboratory may account for the difference. In this paper we investigate parts of the experiment with the one-dimensional turbulence model

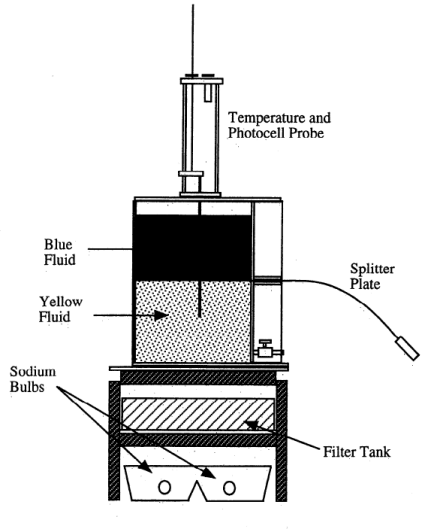

Figure 1. Sketch of the experiment of Sayler and Breidenthal.

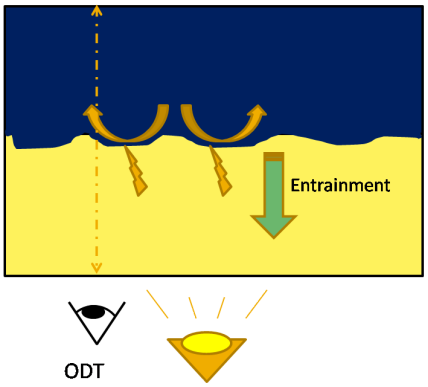

Figure 2. Sketch of the One-dimensional turbulence (ODT) setup.

(ODT), see Fig. 2. In Sec. 2 we summarize the key quantities discussed in the experiment and the assumptions which lead to the equation system to be solved in principle. Sec. 3 summarizes the key idea of ODT and explains how it simplifies the latter equation system to a one-dimensional treatment using map-based advection. Results are given in Sec. 4 and errors of the simulation and the experiment are discussed. We finish with a summary in Sec. 5.

2. Equation system and basic assumptions used to model the experiment

In the following we summarize the key quantities that have been investigated in the experiment. Assumptions to model the experiment are given as well as the final equation system which should be solved in a direct numerical simulation (DNS).

2.1. Investigated quantities

In (Sayler & Breidenthal, 1998) results are given for dimensionless entrainment rates

$$E = \frac{w_e}{w^*}\,. \tag{1}$$

where

$$w_e = \frac{dh}{dt} \tag{2}$$

is the change over time t of the interface height h. The entrainment rate is associated with interfacial convection and has been found to vary inversely with a bulk Richardson number

$$Ri = \frac{g'h}{(w^*)^2}. \tag{3}$$

Here h is the thickness of the convective layer, w^* is a convective velocity scale, and g' is the effective gravity discussed in the next section.

2.2. Mixture density

The fluid density depends on temperature. The initial temperature of the yellow layer, T_l, is $T_u - \Delta T$. The effective gravity can be written in temperature form

$$g' = g\alpha\Delta T, \tag{4}$$

where α is the thermal expansion coefficient of water. These assumptions, which specify the densities of the initial layers, are not exact but they are valid to a good approximation in the Boussinesq regime (small relative variations of thermodynamic variables). This formulation does not explicitly specify the reference density. Instead, a reference temperature, taken to be the initial temperature T_u of the upper (blue) layer, is used. Although temperature varies spatially and temporally, α for a given simulated trial is evaluated at the temperature T_u. A table of α vs. temperature is taken from *http* : *//physchem.kfunigraz.ac.at/sm/Service/Water/H2Othermexp.htm*. On this basis, density is expressed in terms of the temperature variable T which is two-valued initially, but is a continuous function at all later times.

2.3. Radiative heating

Though the LES analog (Bretherton *et al.*, 1999) of the Sayler and Breidenthal (SB) experiment that has been simulated is interpreted as a 'smoke cloud', the laboratory experiment involves transparent and absorbing liquids subject to radiation. The liquid is water containing a dye that is blue (absorbing) for pH>8, yellow (almost transparent) for pH<6, and green in between. The two initial layers contain an acid and a base and so are blue and yellow respectively. The acid and base concentrations determine the equivalence ratio τ defined as the volume of pure basic (yellow) fluid required to neutralize a unit volume of pure acidic (blue) fluid. Here this is interpreted as the crossover from absorbing to transparent. This is an idealization because absorption varies gradually over a range of mixture states, but the dependence of absorption on mixture state is not given in Sayler & Breidenthal (1998), so it cannot be determined without further experimental calibration studies. Absorption is quantified by a length σ such that the ratio of transmitted to incident radiation in a layer of thickness D is $\exp(-D/\sigma)$. For simulation purposes, a mixture fraction χ is used to represent the volume fraction of initially pure acidic fluid in a mixture. Based on the stated idealization, $\chi_s = 1/(1+\tau)$ is the value of χ at which the mixture crosses between the transparent and absorbing states, and it is assumed that σ has the value for pure acidic fluid ($\chi = 1$) if $\chi > \chi_s$, otherwise $\sigma = \infty$ (i.e., no absorption). In reality, σ is a continuous function of χ. If one could determine this functional form, it could be used to improve the physical model of radiative absorption. Three different radiative models are tested in Sec. 4.4. Values for σ and τ for each experimental trial are given in Sayler & Breidenthal (1998). The two initial fluid layers have χ values 0 and 1 respectively, and also have differing densities due to temperature differences. In the experiment, the upper layer is absorbing and its temperature T_u is higher than the temperature of the lower layer (temperature difference ΔT). The two-layer system is radiatively heated from below. Based on the stated assumptions, the radiation flux at a given height is $q_0 \exp(-D/\sigma)$, where q_0 is the source flux and D now represents the total path length through fluid with $\chi > \chi_s$ between the source and the given height.

2.4. The equation system for transport of temperature, composition, and momentum
In the experiment, three diffusive scalar properties, temperature and the concentrations of acid, and base evolve in time, governed (in the Boussinesq approximation) by

$$\begin{aligned} \frac{\partial \mathbf{v}}{\partial t} + \nabla\cdot(\mathbf{v}\circ\mathbf{v}) = &\quad \nu\nabla^2\mathbf{v} + g\alpha(T-T_u)\mathbf{k} \\ \nabla\cdot\mathbf{v} = &\quad 0 \\ \frac{\partial \chi}{\partial t} + \nabla\cdot(\mathbf{v}\chi) = &\quad D_\chi\nabla^2\chi \\ \frac{\partial T}{\partial t} + \nabla\cdot(\mathbf{v}T) = &\quad \kappa\nabla^2 T + S_T(\chi) \end{aligned} \tag{5}$$

The diffusion coefficient D_χ, the kinematic viscosity ν governing the molecular transport of momentum, and the diffusivity of heat κ are all assigned nominal room-temperature values and are given in Table 1. The radiative temperature source term is $S_T(\chi) = \partial_z q(z)$ where $q(z) = q_0 \cdot exp[-(1/\sigma)\int_{-\infty}^{z} H(\chi(z)-\chi_s)dz]$ where H is the Heaviside function and z the vertical coordinate. Since a sequence of direct numerical simulations (DNS) of Eqs. (5) is currently

Table 1. Table of molecular properties and non-dimensional numbers

ν[m^2/s]	κ[m^2/s]	D_χ[m^2/s]	Pr[−]	Sc_χ[−]	Le_χ[−]
1.0e-6	1.43e-7	1.667e-9	7.0	600	86

not affordable, mainly due to the very thin Taylor layers (that are observed in the experiment) compared to the tank size, we solve the system using the one-dimensional turbulence (ODT) model. This method is explained in detail in the next section.

3. The one-dimensional turbulence (ODT) model

3.1. General idea
In ODT Kerstein (1999), the advection process consists of randomly chosen mapping events which are measure-preserving thus fulfilling the second equation in Eq. 5. The mappings rearrange scalar fields which are in the present case temperature, mixture fraction, and the components of velocity on a 1D domain (for affordable resolution of molecular mixing). Each mapping has a certain extension l and end points, z_0 and $z_0 + l$, respectively, and can be seen as the net effect of an eddy of size l acting on the flow. The mapping function is designed to wrinkle the flow by compressing and folding sub-regions within the considered mixing length l. In the presence of gradients the mapping induces a scalar transport which is equivalent to a turbulent flux. The time, location, and length are chosen randomly based on the local energetics of the turbulent field. The time scale can also be interpreted as the turn over time of an eddy of size l. To summarize, the solution procedure in ODT involves two processes, (i) time integration of the 1D form of the equation system (5) excluding the convective terms, and (ii) a sequence of eddy events, which are the instantaneous transformations that represent turbulent stirring. The model has been used in various geophysical applications, among them stable and unstable atmospheric boundary layers Wunsch & Kerstein (2001); Wunsch (2003); Kerstein & Wunsch (2005).

3.2. Advection by triplet maps

Following (Kerstein, 1991), in the spatial continuum, the triplet map is defined as

$$M(z) = z_0 + \begin{cases} 3(z - z_0) & \text{if } z_0 \le z \le z_0 + \frac{1}{3}l \\ 2l - 3(z - z_0) & \text{if } z_0 + \frac{1}{3}l \le z \le z_0 + \frac{2}{3}l \\ 3(z - z_0) - 2l & \text{if } z_0 + \frac{2}{3} \le z \le z_0 + l \\ z - z_0 & \text{otherwise.} \end{cases} \tag{6}$$

Any scalar quantity $S \in [T, \chi, u, v, w]$ which is triplet mapped undergoes the transformation $S(z) \rightarrow S(M(z))$. This mapping takes a line segment $[z_0, z_0 + l]$, shrinks it to a third of its original length, and then places three copies on the original domain. The middle copy is reversed, which maintains the continuity of advected fields and introduces the rotational folding effect of turbulent eddy motion. Property fields outside the size-l segment are unaffected by the map.

4. Results

4.1. Profiles

Some typical snapshots illustrating the time evolution of an ODT run simulating the tank experiment are shown in Fig. 3. The first plot to the left shows the initial conditions where we still have stable conditions since higher temperature (density) is above (below) lower temperature (density). The second plot shows the temperature state shortly after the lamp is switched on. The incoming radiative flux q_0 passes the yellow fluid without absorption. The latter starts when the blue fluid is reached which results in a slightly higher temperature level close to the initially stable front. After a critical Rayleigh number threshold is passed (see third plot) an instability occurs which induces a turbulent state. Finally (last plot to the right), the turbulent state is convected upwards and interacts with the upper free surface condition.

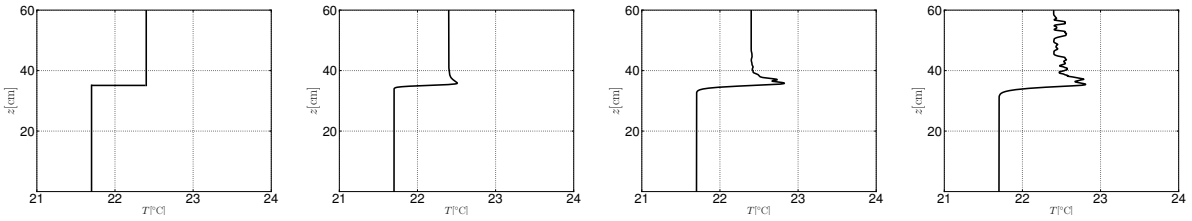

Figure 3. Temperature profiles (plotted over the vertical coordinate) showing the growing of the turbulence in the upper (blue) layer, simulated by the ODT model.

4.2. Entrainment rates

Entrainment rates as a function of Richardson numbers are plotted in Fig. 4 for some numerical and experimental baseline results. Within the statistical precision of these (preliminary) ODT results, they agree with measured entrainment rates and the associated Richardson-number dependences for the heat stratified trials. A small amount of yellow layer absorption has been taken into account to reproduce the experimental results (see radiative model 2 in Sec 4.4). Additional parameter variations indicate sensitivity of the entrainment rate to details such as the opacity dependence on composition.

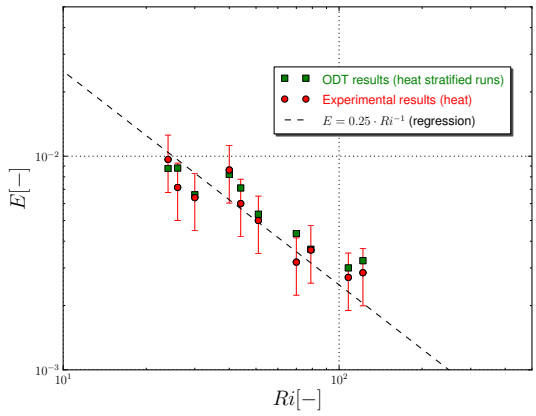

Figure 4. Comparison of entrainment rates for the baseline runs.

4.3. Dependence on the chemical parameter τ

In the experiment the optical absorption is related to the concentration of the basic species. Here, this concentration depends on the chemical reaction at the interface with the acid species in solution in the lower layer fluid. For a certain amount of the reactants all the basic species is consumed by the chemical reaction so that the solution turns yellow. The τ parameter corresponds to the proportion in which the basic and acid reactants have been introduced in the experimental tank and governs the changing of color in the reaction to the mixture fraction of the basic species. Remember that the threshold χ_s, at which the mixture crosses between the transparent and absorbing states, is a function of τ. In the experiment τ is the same for all the trials.

Here we perform a numerical study to test the influence of this parameter on the entrainment rate, all the other parameters remaining unchanged. Figure 5 shows the results of this parametric study for a sample baseline trial. We have chosen case H10 of (Sayler & Breidenthal, 1998) with $\tau = 0.5$. There is a clear influence of the parameter on the evolution of the height h and thus on entrainment w_e results. The greater is τ, the lower is the mixture fraction threshold χ_s, and the greater is E. For lower χ_s absorption takes already place in the diffusion profile, thus turbulence generated by this instability can enter more into the laminar part. This apparently increases entrainment considerably. However, a saturation of this influence is seen after τ of unity is reached. The relative increase of E over the range of investigated τ values is about 50%. Hence τ should be considered as a sensitive parameter in an algebraic entrainment model. The small region of non-monotonicity in Figure 5 is due to the fact that for each run only 9 different samples are considered in the averaged entrainment rates.

4.4. Heating of the lower layer

Parasitical convective motions in the lower layer fluid which were not meant to take place in the experiment are likely to have occurred, and have to be considered to obtain the entrainment values shown in Sec. 4.2. Over the duration of an experimental trial the fluid receives a radiative flux from a sodium light placed under the experimental tank. Ideally absorption of this flux should start in the blue layer, thus passing the bottom of the tank and the yellow layer without considerable loss. Looking at the temperature profiles given in Sayler & Breidenthal (1998) also turbulent motions in the lower layer are recognized. One explanation is that the yellow layer already absorbs some small amount of radiation. Due to the large σ, radiation absorption in the

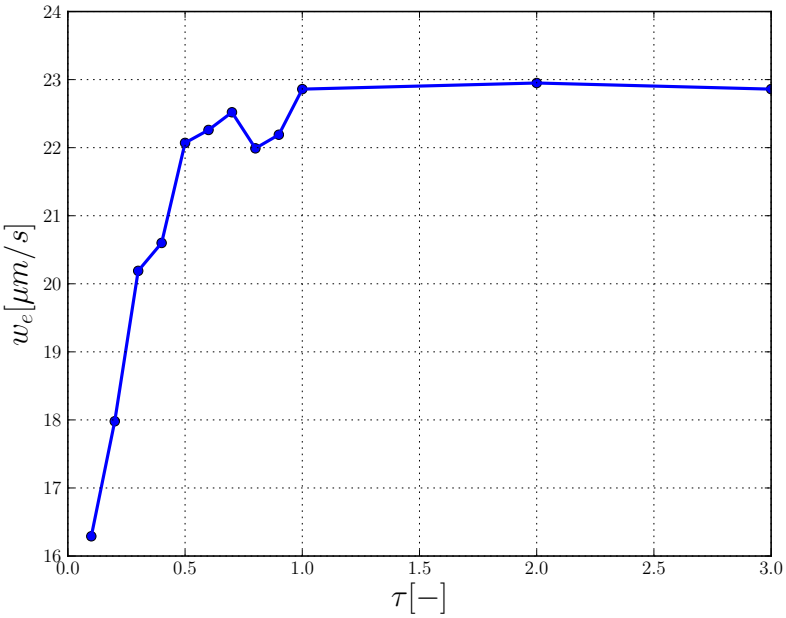

Figure 5. Entrainment rates for several values of τ (trial H10).

yellow layer is only slightly non-uniform, so it might not be the cause of convection in that layer. Another possibility is that the plexiglas is heated by the light and thus heats the fluid near the bottom. However, yellow layer heating causes ΔT to rise more slowly than it otherwise would, so it increases convection for given nominal (initial) Ri. If entrainment is related to Ri at the instant of entrainment, then there might be less or negligible scaled entrainment enhancement.

To investigate the sensitivity of entrainment to the details of the absorption we consider three different hypotheses. Radiation model M1 has zero absorption in the yellow layer and suddenly beginning absorption in the blue. Model M2 takes into account a small amount of heating in the yellow and switches to blue absorption when $\chi \geq \chi_s$. Finally, model M3 behaves like M2, but taking into account a linear relation for the absorption between $\chi < 0$ and $\chi < \chi_s$. The absorption lengths used in the radiative source term S_T for the three cases are summarized as follows:

$$\sigma_{M1} = \begin{cases} \sigma_w & \text{if } \chi < \chi_s \\ \sigma_b & \text{if } \chi \geq \chi_s \end{cases} \tag{7}$$

$$\sigma_{M2} = \begin{cases} \sigma_y & \text{if } \chi < \chi_s \\ \sigma_b & \text{if } \chi \geq \chi_s \end{cases} \tag{8}$$

$$\sigma_{M3} = \begin{cases} \sigma_y & \text{if } \chi = 0 \\ \sigma_y * \frac{\chi_s - \chi}{\chi_s} + \sigma_b * \frac{\chi}{\chi_s} & \text{if } 0 < \chi < \chi_s \\ \sigma_b & \text{if } \chi_s \leq \chi \end{cases} \tag{9}$$

where $\sigma_w = \infty$ (no absorption), $\sigma_y = 60$ cm, $\sigma_b = 1.2$ cm. We use the same trial as for the τ study and average again w_e over 9 runs. The results are shown in Table 2. The radiative model M3 gives the highest entrainment. It is not so surprising that M1 gives the smallest, since only in the upper layer the temperature is increased and thus the stability between upper and lower layer. There is a 100% difference between M1 and M3. More surprising is the considerable difference between M2 and M3, although we the change in the model setup is very small and

restricted to a very thin region ($0 < \chi < \chi_s$) in space. This explains that the uncertainty in the details of radiative absorption easily can explain errors between experiments and simulations. In Fig. 6 results for one run using model M3 is shown. It becomes obvious that also the lower

Table 2. Entrainment rates for three different radiation models.

Rad. model	1	2	3
w_e [μm/s]	10.25	14.05	22.07

layer is heated and that the temperature difference between both layers remains nearly constant throughout a run.

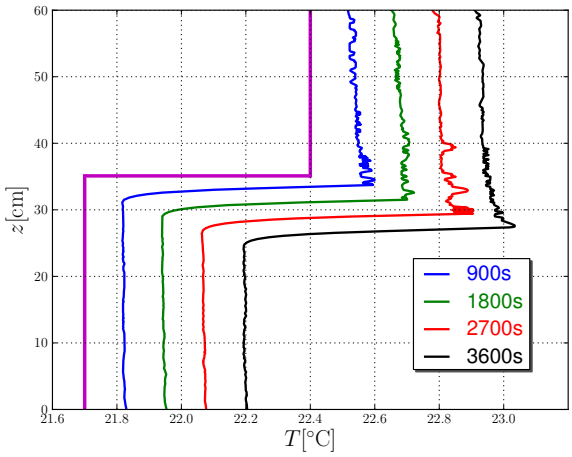

Figure 6. Temperature profile for case H01

5. Summary

The key results of the current ODT simulations are stated in the following:

- Assuming a small amount of yellow layer absorption to represent heating effects in that layer that are not fully characterized, measured entrainment over a range of Richardson numbers is reproduced.
- Considerable differences in the entrainment rates are obtained when using slightly different radiative models.
- The chemical parameter τ plays a non-negligible role for the entrainment.

6. Acknowledgement

The work was partially supported by the the German Science Foundation under Grant SCHM-1682/4. Partially supported by the Department of Energy Laboratory Directed Research and Development (LDRD) program at Sandia National Laboratories. Sandia National Laboratories is a multi-program laboratory operated by Sandia Corporation, a Lockheed Martin Company, for the United States Department of Energy under contract DE-AC04-94-AL85000.

References

Bretherton, Christopher S., MacVean, Malcolm, Bechtold, Peter, Chlond, Andreas, Cotton, William, Cuxart, Joan, Cuijpers, Hans, Khairoutdinov, Marat, Kosovic, Bronko, Lewellen, Dave, Moeng, Chin-Hoh, Siebesma, Pier, Stevens, Bjorn, Stevens, Dave, Sykes, Ian & Wyant, Matt 1999 An intercomparison of radiatively-driven entrainment and turbulence in a smoke cloud, as simulated by different numerical models. *Quart. J. Roy. Meteor. Soc.* **125**, 391–423.

Kerstein, A. R. 1991 Linear-eddy modelling of turbulent transport. Part 6. Microstructure of diffusive scalar mixing. *J. Fluid Mech.* **231**, 361–394.

Kerstein, A. R. 1999 One-dimensional turbulence: Model formulation and application to homogeneous turbulence, shear flows, and buoyant statistical flows. *J. Fluid Mech.* **392**, 277–334.

Kerstein, A. R. & Wunsch, S. 2005 Simulation of a stably stratified atmospheric boundary layer using one-dimensional turbulence. *Bound. Layer Meteorol.* **118**, 325–356.

McEwan, A. D. & Paltridge, G. W. 1976 Radiatively driven thermal convection bounded by an inversion – a laboratory simulation of stratus clouds. *J. Geophys. Res.* **81**, 1095–1102.

Sayler, B. J. & Breidenthal, R. E. 1998 Laboratory simulations of radiatively induced entrainment in stratiform clouds. *J. of Geophys. Res.* **103**, 8827–8837.

Wunsch, S. 2003 Stochastic simulations of buoyancy reversal experiments. *Phys. Fluids* **15**, 14421456.

Wunsch, S. & Kerstein, A. 2001 A model for layer formation in stably-stratified turbulence. *Phys. Fluids* **13**, 702–712.